

STAGNATION-POINT RADIATIVE HEAT FLUXES IN NEPTUNE AEROCAPTURE

Chul Park

*Department of Aerospace Engineering, Korea Advanced Institute of Science and Technology
373-1 Guseong-dong, Yuseong-gu, Daejeon, 305-701, South Korea, cpark216@kaist.ac.kr*

ABSTRACT

The radiative heat flux incident on the edge of the boundary layer at the stagnation point of a spacecraft entering into Neptune is calculated approximately. The atmosphere of Neptune is assumed to consist of a 81% H₂-19% He mixture. The flow along the stagnation streamline is represented by a one-dimensional inviscid flow in a constant-area channel. A technique recently developed by the author is applied to determine the radiative heat flux reaching the end of a 1 cm gas slug in this constant-area tube. A blunted double cone entry vehicle of $L/D = 0.88$ with a nose radius of 0.2 m and ballistic coefficient of 609 kg/m² is assumed to fly an aero-braking trajectory in retrograde direction. Entry velocities of 31, 29, 27, and 25 km/s are calculated to produce radiative heat loads of 84, 172, 49, and 22 kJ/cm².

1. INTRODUCTION

Humans have succeeded in entering the atmosphere of the planet Jupiter in the Galileo Probe mission. But the other outer planets, Saturn, Uranus, and Neptune, are yet to be explored. Of these, Neptune has drawn some interest already [1,2]. In Neptune entry, Ref. [1] shows that the peak heating occurs when the stagnation pressure is about 1 atm. The shock layer flow is likely to be in a thermochemical nonequilibrium state. Neptune's atmosphere consists of 81% H₂, about 18% He, and a small concentration of other gases, mostly CH₄ [3]. The anticipated entry velocities vary up to about 30 km/s. In Ref. [1], the nonequilibrium flow conditions were calculated using a chemistry model derived from the information generated prior to 1990.

The most crucial part of the chemistry model used in Ref. [1] concerns ionization rate of atomic hydrogen. The model is from the shock tube experiment of Leibowitz [4] of 1973. In 1976, Livingston and Poon [5] carried out another shock tube experiment. Both these experiments measured the time needed to reach ionization equilibrium in hydrogen. There was up to a factor three difference in the ionization times determined by these two groups: Livingston and Poon's times were longer. In Livingston and Poon's work, absolute value of the peak electron density was

measured. Surprisingly, the measured electron density was higher than the equilibrium value.

Howe [6] reasoned that H should ionize mostly by the collisions of electrons. Because one electron-impact ionization produces one additional electron, this process increases ionization level exponentially. Therefore the ionization should occur suddenly, in a process known as avalanche ionization. Howe believed that significant radiation occurs only when H-atoms are ionized. And so, in the region upstream of this avalanche ionization, radiation emission should be nearly zero. Avalanche ionization drives the chemical state to ionization equilibrium, and so the region downstream of ionization will emit equilibrium radiation. This reasoning leads to the conclusion that the delay of ionization due to nonequilibrium generally reduces the radiative heat transfer rate to an entry vehicle.

Very recently, Park [7] analyzed both Leibowitz's and Livingston and Poon's experimental data. Park concluded that the data of Leibowitz may have been in error. The error was likely caused by the influence of the radiation emitted by the driver gas absorbed by the test gas. From the work of Livingston and Poon, Park derived a comprehensive thermochemical model for ionization of hydrogen-helium mixtures. Park's model reproduces both experimental data, and enables one to calculate radiation intensity in a hydrogen-helium mixture under a nonequilibrium condition. Park then applied this model to one entry trajectory considered by Jits et al.

It is the purpose of the present work to apply Park's method to a wider range of Neptune entry conditions.

2. PARK'S MODEL

From the existing experimental and theoretical data, Park [7] reasoned that the temperature of electrons and the vibrational temperature of H₂ will be strongly coupled. The latest work by Kim et al [8,9] show that, during the dissociation of H₂ by the collisions of H, H₂, and He, rotational temperature is not in equilibrium with the translational temperature. However, a two-temperature description is still valid in describing the process of dissociation of H₂ provided the rate

coefficients are properly chosen. Thus, a two-temperature model can be derived in which vibrational, electron, and electronic temperature is one temperature and translational temperature is another temperature.

In the work of Park [7], these latest works of Kim et al [8,9] were used in describing the process of dissociation of H_2 in the presence of H, H_2 , and He. Ionization of H is considered to occur by the collisions of electrons, H, and He. Eight rate coefficients were derived to describe the ionization in this situation, which are functions of the heavy particle temperature, vibrational-electron-electronic temperature, number density of H and He, and the extent of absorption of radiation by the Lyman- α line of H at 1216 Å [10]. The extent of absorption of Lyman- α line was calculated in turn by integrating the radiative transfer equation through the entire medium including the freestream.

The crucial unknown parameter in describing the ionization process in a H_2 -He mixture is the cross section for excitation of H by the collisions of H and He. Leibowitz [4] determined the cross section to be $4 \times 10^{-17} \text{ cm}^2$ from his experiment.

In 2002, Bogdanoff and Park [11] carried out an experiment in a shock tube similar to that used by Leibowitz [4]. They saw that ionization equilibration occurred much earlier than predicted by Leibowitz's model and the level of ionization was much larger than the equilibrium value. By analyzing the radiation travelling along the shock tube, they found that the radiation emitted by the hot driver gas was responsible for this phenomenon.

The shock tube used by Bogdanoff and Park [11] and that by Leibowitz [4] were both driven by an electric-arc heated driver gas. In the latest work of Park [7], Leibowitz's data is not used in deducing the cross section. Instead, the results by Livingston and Poon [5] were used. Livingston and Poon used a shock tube which was driven by a magneto-hydrodynamic force. As such, strong irradiation by the drive gas was not likely.

From the data of Livingston and Poon, the ionization cross section of H and He was deduced by Park [7] to be $1 \times 10^{-17} \text{ cm}^2$. Fig. 1 compares the experimental data of Livingston and Poon with Park's model. The peak electron density values calculated by Park are compared with experimental data in Fig. 2. As seen, fairly good agreement was obtained.

In order to numerically reproduce the experimental data by Leibowitz [4], Park assumed that the driver gas was irradiating as a black body. The assumed driver temperature was varied until the measured

equilibration distance was reproduced. In Fig. 3, the influence of the driver irradiation is shown.

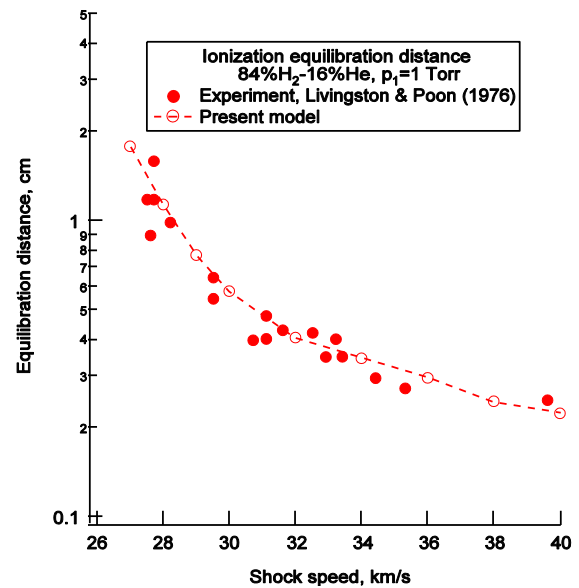


Fig. 1. Equilibration distance in the experiment by Livingston and Poon [5].

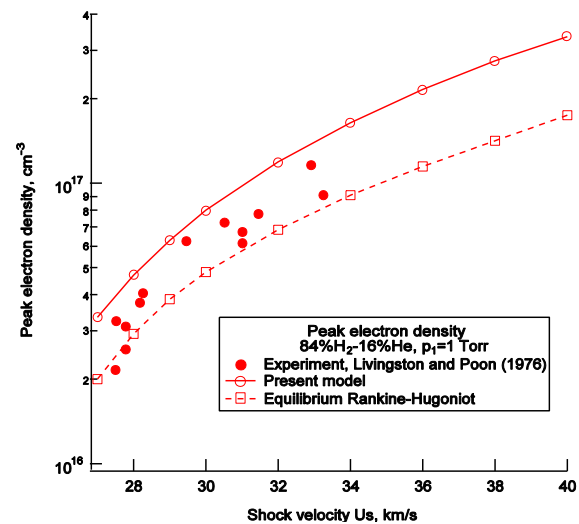


Fig. 2. Peak electron density in the experiment by Livingston and Poon [5].

By choosing the driver temperature appropriately, the experimental data on the variation in continuum radiation intensity obtained by Leibowitz can be reproduced, as shown in Fig. 4. The equilibration distance obtained by Leibowitz can be reproduced also by choosing appropriate values of driver temperature as shown in Fig. 5.

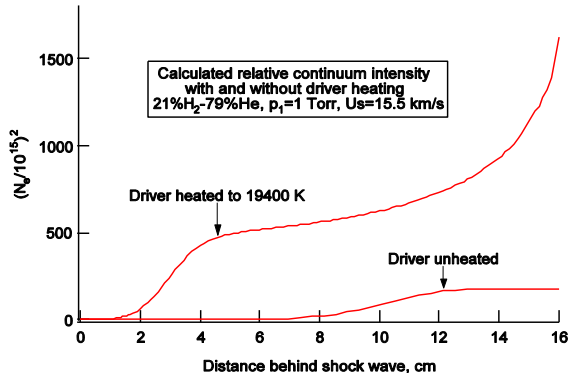


Fig. 3. Effect of driver irradiation on ionization level and equilibration distance.

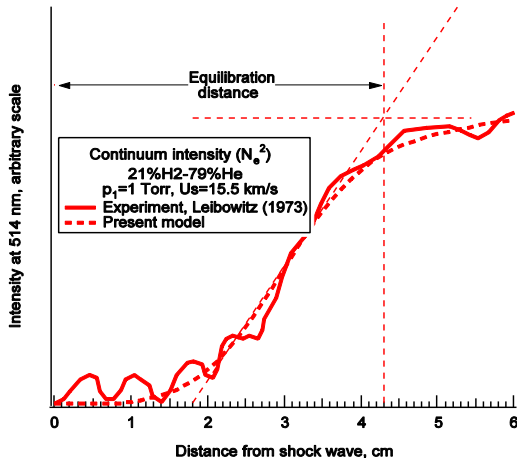


Fig. 4. Variation of continuum radiation intensity obtained by Leibowitz [4] and Park's calculation.

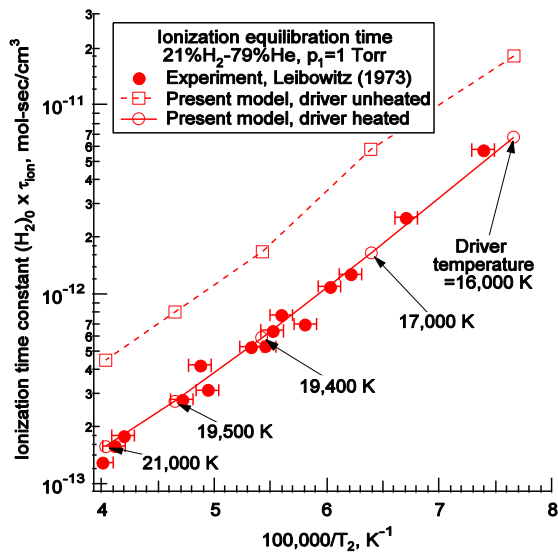


Fig. 5. Equilibration distance obtained by Leibowitz [4] and Park's model.

In Fig. 5, one sees a factor of three difference in equilibration distances between that with driver radiation and that without. Thus the difference between the two sets of data is now reconciled by accounting for the driver irradiation. The ionization cross section value of $4 \times 10^{-17} \text{ cm}^2$ obtained by Leibowitz, four times larger than the $1 \times 10^{-17} \text{ cm}^2$ obtained by Park [7], reflects this factor three higher equilibration rate.

As Fig. 4 shows, ionization of H is rather gradual and does not occur in an avalanche fashion. As will be shown later, radiation occurs not only in the downstream region where ionization level is high but also in the upstream region where ionization level is low. This phenomenon invalidates the theory of Howe [6].

3. METHOD OF CALCULATION

Jits et al considered a blunted double cone flying in Neptune to aero-brake the vehicle so that it is inserted into an elliptic orbit that approaches Neptune's moon Triton. The entry flight occurs in the retrograde direction because Triton's orbital motion is retrograde with respect to the rotation of Neptune. The vehicle has a mass of 600 kg, base diameter of 1 m, and a ballistic coefficient of 609 kg/m^2 . The vehicle performs a sophisticated roll modulation to minimize heat load. Table 1 summarizes the convective and radiative heat loads calculated by Park [7] for this trajectory.

Table 1. Flight environments of Jits et al (2003) trajectory.

Flight time sec	Freestream density kg/m^3	Flight velocity m/s	q_{conv} kW/cm^2	q_{rad} kW/cm^2
154	1.95^{-5}	31373	0.921	0.0805
164	4.95^{-5}	30996	1.42	0.259
174	1.11^{-4}	30090	1.95	0.481
184	1.57^{-4}	28608	1.99	0.357
194	1.38^{-4}	27118	1.59	0.118
204	8.32^{-5}	26125	1.20	0.026

The same vehicle is considered in the present work. However, the roll modulation is drastically simplified, and optimization is not sought. Four entry velocities, 31, 29, 27, and 25 km/s, are considered. The vehicle is assumed to fly with the lift vector pointing downward at high altitudes, and upward at low altitudes. The switching occurs at 135 km altitude for the 31 km/s entry, 140 km for the 29 km/s entry, 160 km for the 27 km/s entry, and 200 km altitude for the 25 km/s entry. The freestream densities and flight velocities are listed in Tables 2(a) through (d).

Table 2. Flight environments of the present work. (a) Entry velocity = 31 km/s.

Flight time sec	Freestream density kg/m ³	Flight velocity m/s	q_conv kW/cm ²	q_rad kW/cm ²
143	3.06 ⁻⁶	33733	0.451	0.160
153	6.57 ⁻⁶	33700	0.661	0.204
163	1.40 ⁻⁵	33617	0.968	0.587
173	3.11 ⁻⁵	33429	1.427	1.089
183	7.54 ⁻⁵	32989	2.158	2.252
193	2.16 ⁻⁵	31853	3.327	1.871
203	3.57 ⁻⁵	29525	3.415	1.324
213	2.61 ⁻⁴	27362	2.307	0.495
223	1.14 ⁻⁴	26286	1.335	0.109
233	5.54 ⁻⁵	25831	0.880	0.052
243	3.03 ⁻⁵	25598	0.630	0.042

Table 2. (b) Entry velocity = 29 km/s

Flight time sec	Freestream density kg/m ³	Flight velocity m/s	q_conv kW/cm ²	q_rad kW/cm ²
172	2.96 ⁻⁶	31750	0.352	0.127
182	5.10 ⁻⁶	31725	0.463	0.200
192	8.68 ⁻⁶	31676	0.603	0.322
202	1.43 ⁻⁵	31590	0.772	0.483
212	2.38 ⁻⁵	31444	0.974	0.716
222	4.04 ⁻⁵	31198	1.262	1.013
232	7.26 ⁻⁵	30774	1.633	1.640
242	1.43 ⁻⁴	29992	2.133	1.110
252	2.03 ⁻⁴	28729	2.244	0.831
262	1.76 ⁻⁴	27447	1.818	0.546
272	1.04 ⁻⁴	26600	1.266	0.164

Table 2. (c) Entry velocity = 27 km/s.

Flight time sec	Freestream density kg/m ³	Flight velocity m/s	q_conv kW/cm ²	q_rad kW/cm ²
202	7.22 ⁻⁶	29928	0.465	0.215
214	1.34 ⁻⁵	29848	0.633	0.359
226	2.54 ⁻⁵	29692	0.861	0.580
238	5.07 ⁻⁵	29388	1.186	0.850
250	9.72 ⁻⁵	28786	1.552	0.981
262	1.30 ⁻⁴	27862	1.632	0.680
274	1.13 ⁻⁴	26931	1.367	0.278
286	6.90 ⁻⁵	26291	0.991	0.088

Table 2. (d) Entry velocity = 25 km/s.

Flight time sec	Freestream density kg/m ³	Flight velocity m/s	q_conv kW/cm ²	q_rad kW/cm ²
220	4.12 ⁻⁶	27986	0.287	0.095
235	8.14 ⁻⁶	27940	0.403	0.151
250	1.57 ⁻⁵	27838	0.557	0.221
265	2.93 ⁻⁵	27638	0.747	0.296
280	4.60 ⁻⁵	27293	0.905	0.282
295	5.55 ⁻⁵	26828	0.945	0.189
310	4.96 ⁻⁵	26358	0.846	0.098

325	3.45 ⁻⁵	25995	0.674	0.059
340	2.04 ⁻⁵	25765	0.503	0.046

4. RESULTS

4.1. General Features of Solutions

The general features of the solutions are shown for the 232 sec time point in the 29 km/s entry, in Figs. 6(a) to (c), 7, and 8. As Fig. 6(a) shows, both heavy particle temperature and vibrational-electron-electronic temperature are discernibly higher than the equilibrium temperature within the first 1 cm. Fig. 6(b) shows that H⁺ increases gradually: no avalanche ionization is observed.

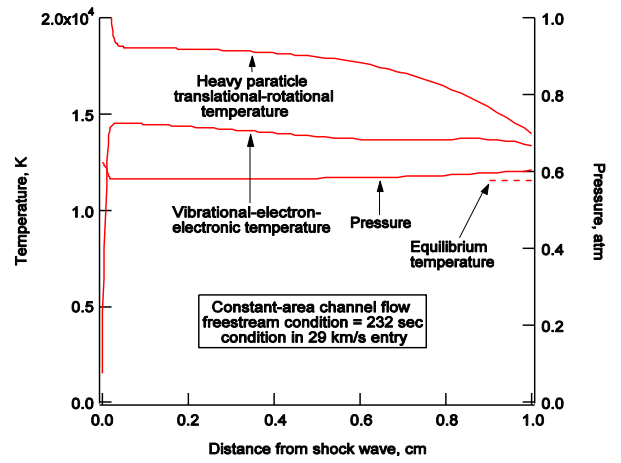


Fig. 6. Flow conditions for the 232 sec point in the 29 km/s entry. (a) Temperatures and pressure.

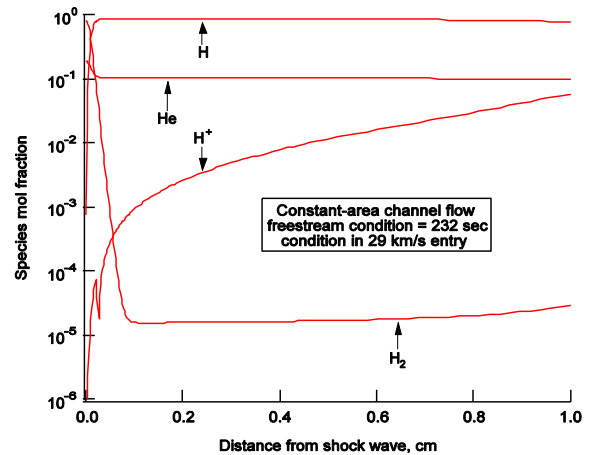


Fig. 6. (b) Species mol fractions

In Fig. 6(c), the radiative heat fluxes in the downstream and upstream directions and the radiative heating rate (power gain by the gas by absorbing radiation) are shown. Roughly, the downstream-directed radiative

heat flux increases linearly with distance. More precisely, the rate of increase is the largest immediately behind the shock wave, and decreases toward the downstream. Immediately behind the shock wave, the B-X and C-X bands of H_2 are radiating strongly. As soon as H_2 is dissociated, the collisions of H and He quite effectively excite H to emit radiation. This is also opposite of what was postulated by Howe [6]. Radiative heating rate is mostly negative, signifying that the gas is being cooled rather than heated, i.e., emission rather than absorption is dominant. The magnitude of the rate is considerable.

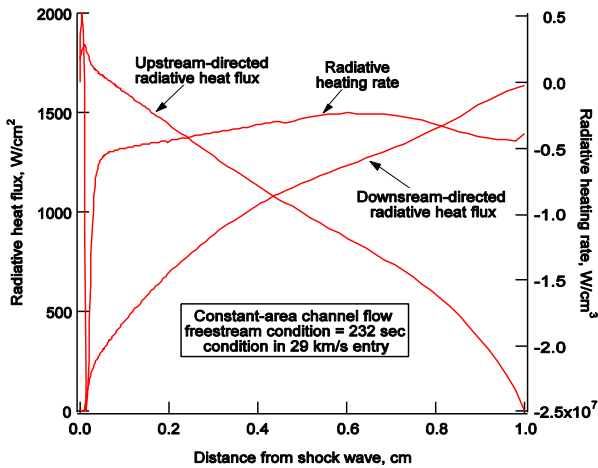


Fig. 6. (c) Radiative heat flux and radiating heat rate.

In Fig. 7, the spectrum of the radiation is shown at the 1 cm point. As seen, the five components of radiation, lines, Lyman and Balmer continua, and the B-X and C-X bands of H_2 , all contribute more or less to the same order of magnitude.

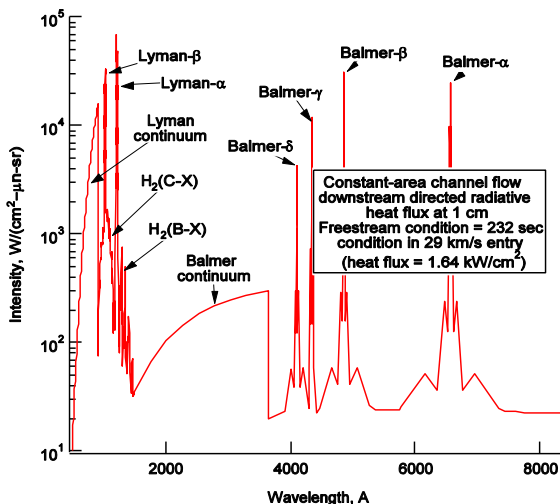


Fig. 7. Spectral intensity of the normal ray facing into the downstream direction at 1 cm from the shock wave for the 232 sec point in the 29 km/s entry.

In Fig. 8, the precursor phenomena is shown. Species H and H_2^+ are produced by absorption of the Lyman continuum. Vibrational-electron-electronic temperature rises to about 1600 K, because of the absorption of the B-X and C-X bands of H_2 .

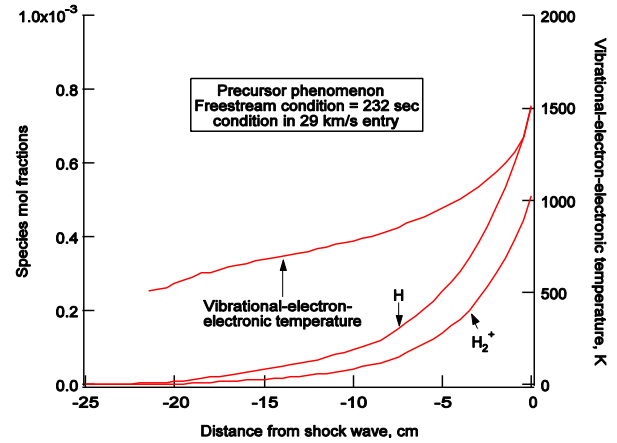


Fig. 8. Precursor phenomenon for the 232 sec point in the 29 km/s entry.

4.2. Heat Transfer Rates

In Fig. 9, the stagnation pressure is shown for the four entry flights considered in the present work and the flight considered by Jits et al [2]. The 29 km/s entry considered in the present work produces stagnation pressures that are roughly the same as those considered by Jits et al.

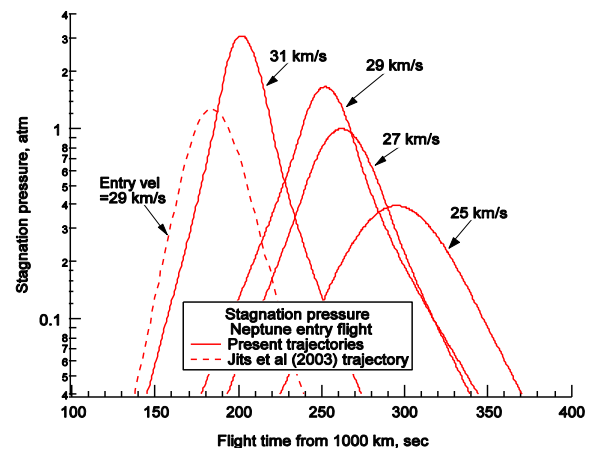


Fig. 9. Stagnation pressures for the calculated entry flights.

In Fig. 10, the convective heat transfer rates to the stagnation point are shown. These values are listed also in Tables 2(a) through (d). As seen, for the present 29 km/s entry, the calculated heat transfer rates are roughly the same as those by Jits et al.

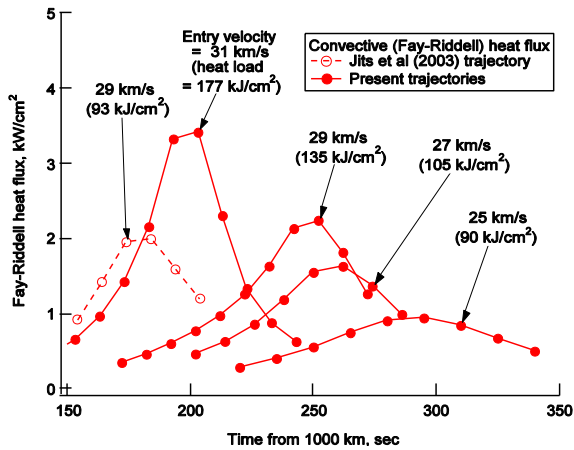


Fig. 10. Convective heat transfer rates in the Neptune entries calculated by the method of Fay and Riddell.

In Fig. 11, the radiative heat fluxes at the 1 cm point are shown. These values are listed in Tables 2(a) through (d) also. The radiative heat loads, i.e., the time integration of the radiative heat fluxes, are indicated in the figure. As seen, the present 29 km/s entry case shows slightly higher heat load compared with Jits et al's case. The peak radiative heating rate for the 29 km/s entry reaches a value of some 1.6 kW/cm².

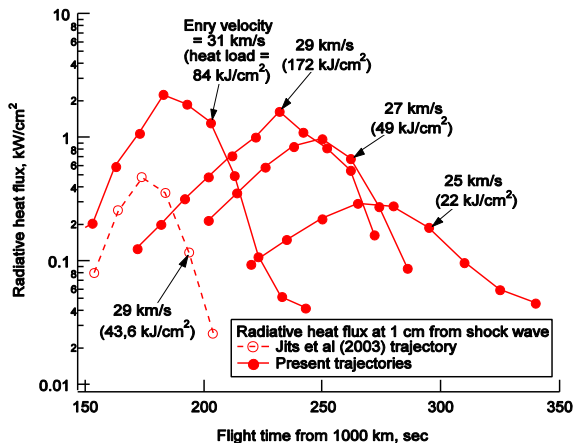


Fig. 11. Radiative heat fluxes in Neptune entries.

5. CONCLUSIONS

In the aero-braking entry flights into the planet Neptune presently with an entry vehicle of 0.2 m nose radius, radiative heat transfer rates become smaller than convective heat transfer rates. The peak radiative heating rate for the 29 km/s entry reaches a value of about 1.6 kW/cm². For a 29 km/s entry, the peak radiative heating rate approaches 1.6 kW/cm² and the heat load approaches 172 kJ/cm².

6. REFERENCES

- Hollis, B. R., Wright, M. J., Olejniczak, J., Takashima, N., Sutton, K., and Prabhu, D. Preliminary Convective-Radiative Heating Environments for a Neptune Aerocapture Mission. AIAA Paper 2004-5177, 2004.
- Jits, R., Wright, M., and Chen, Y-K. Closed-Loop Trajectory Simulation for Thermal Protection System Design for Neptune Aerocapture. *Journal of Spacecraft and Rockets*, Vol. 42, 1025-1034. 2005.
- Gautier, D., Conrath, B. J., Owen, T., de Pater, I., and Atreya, S. K. The Troposphere of Neptune. in *Neptune and Triton*, edited by D. P. Cruikshank, The University of Arizona Press, Tucson, Arizona, 547-610, 1995
- Leibowitz, L. P. Measurement of the Structure of Ionizing Shock Wave in a Hydrogen-Helium Mixture. *The Physics of Fluids*, Vol. 16, 59-68, 1973.
- Livingston, F. R., and Poon, T. Y. Relaxation Distance and Equilibrium Electron Density Measurements in Hydrogen-Helium Plasmas. *AIAA Journal*, Vol. 14, 1335-1337, 1976.
- Howe, J. T. Hydrogen Ionization in The Shock Layer for Entry Into The Outer Planets. *AIAA Journal*, Vol. 12, 876-876, 1974.
- Park, C. Nonequilibrium Ionization and Radiation in Hydrogen-Helium Mixtures, AIAA Paper 2010-814, 2010; submitted to *Journal of Thermophysics and Heat Transfer*.
- Kim, J. G., Kwon, O. J., and Park, C. Master Equation Study and Nonequilibrium Chemical Reactions for H + H₂ and He + H₂. *Journal of Thermophysics and Heat Transfer*, Vol. 23, 443-453, 2009.
- Kim, J. G., Kwon, O. J., and Park, C. State-to-State Rate Coefficients and Master Equation Study for H₂+H₂. AIAA Paper 2009-1023; to be published in *Journal of Thermophysics and Heat Transfer*.
- Park, C. Effect of Lyman Radiation on Nonequilibrium Ionization of Atomic Hydrogen. AIAA Paper 2004-2277, 2004.
- Bogdanoff, D. W., and Park, C. Radiative Interaction Between Driver and Driven Gases in an Arc-Driven Shock Tube. *Journal of Shock Wave*, Vol. 12, 205-214, 2002